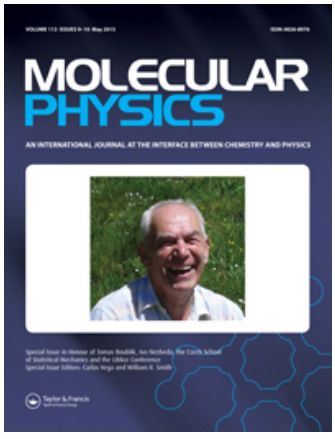

Molecular Physics: An International Journal at the Interface Between Chemistry and Physics
Publication details, including instructions for authors and subscription information:
http://www.tandfonline.com/loi/tmph20

Liquid crystal phase diagram of soft repulsive rods and its mapping on the hard repulsive reference fluid

Alejandro Cuetos[a] & Bruno Martínez-Haya[a]
[a] Department of Physical, Chemical and Natural Systems, Universidad Pablo de Olavide, Seville, Spain
Published online: 13 Jan 2015.

To cite this article: Alejandro Cuetos & Bruno Martínez-Haya (2015) Liquid crystal phase diagram of soft repulsive rods and its mapping on the hard repulsive reference fluid, Molecular Physics: An International Journal at the Interface Between Chemistry and Physics, 113:9-10, 1137-1144, DOI: 10.1080/00268976.2014.996191

To link to this article: http://dx.doi.org/10.1080/00268976.2014.996191

Molecular Physics, 2015
Vol. 113, Nos. 9–10, 1137–1144, http://dx.doi.org/10.1080/00268976.2014.996191

INVITED ARTICLE

Liquid crystal phase diagram of soft repulsive rods and its mapping on the hard repulsive reference fluid

Alejandro Cuetos* and Bruno Martínez-Haya

Department of Physical, Chemical and Natural Systems, Universidad Pablo de Olavide, Seville, Spain

(*Received 2 November 2014; accepted 3 December 2014*)

The liquid crystal phase diagram of the soft repulsive Kihara fluid has been characterised by means of Monte Carlo simulations, for a selection of elongations of the rod-like particles (L^*= 2–7) and over a broad range of temperatures (T^*= 1–50). Three qualitatively different regimes of liquid crystalline behaviour are described that are related to the emergence of isotropic–nematic–smectic and isotropic–smectic–solid triple points above specific rod elongations. A mapping of the soft repulsive fluids on hardrepulsive fluids of effective elongation depending on L^* and T^* is evaluated. Such mapping provides a correct qualitative description of the role of temperature on the liquid crystal phases, and provides a fairly accurate prediction of equations of states and radial functions within the isotropic, nematic and smectic phases. Nevertheless, in comparison to the simulation results, the mapping underestimates the temperature of the isotropic–nematic–smectic triple point, while it overestimates that of the isotropic–smectic–solid one. These results should guide the use of reference hard-body systems to describe the behaviour of soft liquid crystalline materials.

Keywords: hard spherocylinder; soft spherocylinder; phase diagram; Tomas Boublick; liquid crystals; perturbation theory; computer simulation

1. Introduction

The determination of equations of state (EOS) and phase diagrams for suitable models of molecular fluids constitutes one of the major challenges of statistical mechanics. This is typically a difficult task, which is only affordable in an accurate way for simplified models that are usually conformed of particles with hard-body interactions. Hard-body models serve to characterise real colloidal fluids in certain limiting cases and constitute valid benchmarks for the description of fundamental properties including phase transitions. Moreover, hard-body fluids are commonly employed as reference models in perturbation theories, leading to one the most fruitful tools for the thermodynamic characterisation of complex fluids [1,2].

The main idea behind perturbation theories is to reproduce the relevant intermolecular interactions of the fluid in terms of a reference repulsive potential plus a comparably small short-range attractive perturbation. For potentials with spherical symmetry, a vast body of work over the past decades has been based on perturbative approaches with the hard-sphere (HS) model as reference system. Indeed, the HS system can be regarded as the simplest fluid model beyond the trivial case of the ideal gas, and its thermodynamic behaviour is well characterised [3,4]. In a classic extension of this approach, Chandler, Weeks and Anderson (CWA theory) [5] introduced the possibility of employing a soft repulsive potential as reference, with the fundamental advantage of being completely derivable.

Early advances in perturbation formalisms for the more general case of fluids involving non-spherical particles were achieved in the 1970s and 1980s [6–13]. Tomas Boublik was one of the main scientists pioneering these developments and was part of the team that performed the first simulation studies on these systems [14,15], thereby contributing to the understanding of the thermodynamic behaviour of fluids of hard convex bodies and of their mixtures with spherical particles [16–18]. Of particular relevance to the present work, Boublik was involved in the evaluation of the Kihara potential for rod-like particles [8–11,19], on which the soft repulsive potential employed in the present work is based.

The treatment of fluids of non-spherical particles is largely complicated by the rotational degrees of freedom and by the intrinsic anisotropy of the pair interactions. These fundamental difficulties are however compensated for by the emergence of a new phenomenology. In particular, the phase diagram of these fluids is qualitatively enriched by the so-called liquid crystalline phases, featuring orientational order but a significant degree of positional fluid-like disorder [20].

Most of the theoretical studies on fluids of anisotropic particles have been restricted to small aspect ratios for

* Corresponding author. Email: acuemen@upo.es

which liquid crystalline phases are actually not stable. Those studies have rather focused on general aspects of gas–liquid–solid phase equilibrium and transport properties. The theoretical treatment of mesophasic fluids of particles with greater particle anisotropies was pioneered by Onsager [21] and has developed over time through a number of theoretical approaches [22,23]. Nevertheless, computer simulation constitutes still nowadays the primary tool for the study of these systems. Some of the main benchmark rigid-body molecular models employed over the past decades to describe liquid crystals are the hard ellipsoid (HE) model [24], the Gay–Berne (GB) model [25–27], and the Kihara-type models, such as the hard spherocylinder (HSC) model [22,28] and its soft-interacting variants [29]. The liquid crystalline behaviour of these models has been extensively studied, for both prolate (rod-like) and oblate (disc-like) particle shapes and interaction anisotropies.

This paper is devoted to one of the fundamental Kihara models, namely the soft repulsive spherocylinder (SRS) model, applied in particular to rod-like particles [30–35]. The SRS model is built from the truncation of the 12-6 Kihara potential, in a similar way as it is done in the CWA theory for the Lennard-Jones potential [1,5]. Consequently, the SRS model can be expected to provide an adequate reference potential in perturbation theories of liquid crystal fluids. In addition, since the SRS model is fully derivable, it is suitable for dynamical studies [36]. This is in contrast to the HSC model, which requires complex approximate methods to estimate forces and momentum exchanges. In spite of these potentialities, the SRS fluid has been scarcely investigated in comparison to the HE, HSC and GB models, or even to other Kihara models. Earl and co-workers [33], Aoki and Akiyama [30,31], as well as our group [34,35] have studied the phase behaviour of rod-like SRS particles of elongation $L/\sigma = 4$ and 5, confirming the existence of nematic and smectic A liquid crystal phases, along with the limiting cases of the isotropic and solid phases at low and high density, respectively. Those studies laid out a series of questions that remain to be explored. For instance, in the HSC model, the stability of the different mesophases depends on the aspect ratio of the particles [28] and on the density of the system, while temperature does not play an explicit role. The soft repulsive interaction potential of the SRS model incorporates temperature as a key physical parameter of the system that can modulate the phase diagram giving rise to coexistences and triple points. The rationalisation of these features becomes essential if the SRS model is to be taken as reference potential for realistic fluids and if it is to be employed in molecular dynamics methodologies.

In this study, we have carried out a systematic characterisation of the liquid crystal phase diagram of the SRS fluid by means of isothermal–isobaric Monte Carlo (MC) simulations, encompassing an ample range of particle aspect ratios ($L/\sigma =$ 2–7). Complementing the computer simulations, we have evaluated the performance of a mapping of the phase diagram of the SRS system in terms of that of the HSC model derived by Bolhuis and Frenkel from free –energy calculations [28]. In doing this, we have taken advantage of the original idea introduced by Boublik of finding effective hard potentials to describe the behaviour of soft potentials at given temperatures [10].

Details about the methodologies employed and a summary of the results are provided in the following sections. The MC study shows evidence for the existence of isotropic–nematic–smectic and isotropic–smectic–solid triple points, and serves to estimate their location in terms of density, temperature and particle elongation. It is also shown that the mapping approach provides a fairly accurate description of the liquid crystal phase diagram of the SRS fluid with only HSC data as input.

2. Methodology

2.1. The SRS model potential

The interaction potential of the SRS fluid is built from the truncation and shift of the 12-6 Kihara potential to retain its soft repulsive wall [34,35]. Its associated mathematical expression is

$$U_{\mathrm{SRS}} = \begin{cases} 4\epsilon\left[(\sigma/d_m)^{12} - (\sigma/d_m)^6 + 1/4\right] & d_m \leq \sqrt[6]{2}\,\sigma \\ 0 & d_m > \sqrt[6]{2}\,\sigma \end{cases}$$

where d_m is the minimum distance between segments of length L that describe the cores of the interacting molecules; d_m depends on the relative positions and orientations of the molecules [37]. Hence, the spherocylinder shape of the SRS molecules can be described by an elongation $L^* = L/\sigma$, where the diameter of the molecule, σ, is associated to the range of the pair potential [35]. The inset of Figure 1 represents a pair of interacting rods and aids to visualise these geometrical parameters. In addition, ϵ modulates the strength of the repulsive interaction and is reminiscent of the related role that it plays in the original 12-6 Kihara model. When comparing Kihara-type potentials (such as the SRS model) with ellipsoidal potentials (e.g. the HE and GB models), it must be noted that the aspect ratio of ellipsoidal molecules is actually equivalent to the ratio $(L+\sigma)/\sigma = L^*+1$ of the spherocylinders (see e.g. Figure 1 of [38]).

2.2. SRS–HSC mapping

Barker and Henderson [2] proposed a methodology to describe the thermodynamical and structural properties of fluids from hard-body reference potentials. Boublik extended later this approach to molecular fluids [10]. Basically, a soft repulsive potential is replaced by an effective hard-body potential with a temperature-dependent effective size. In

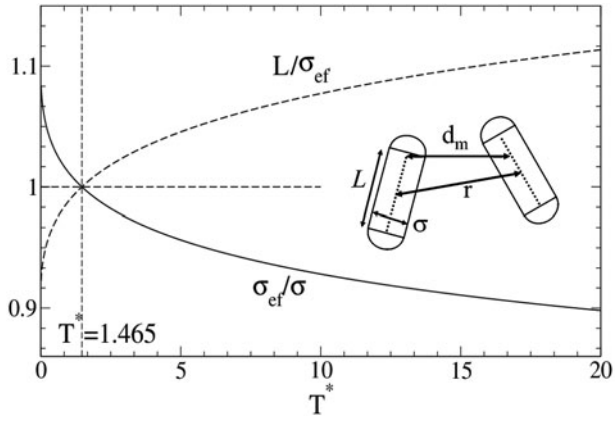

Figure 1. Inset: representation of two Kihara rod-like particles, indicating the relevant geometrical parameters determining their shape (length, L, and diameter, σ) and pair interactions (minimum distance between cores, d_m). Main graph: temperature dependence of the effective molecular diameter, σ_{ef}, assigned by Equation (2) to the HSC reference potential mapping the SRS fluid. Note that σ_{ef} decreases with temperature due to the enhanced interpenetration of the soft interacting particles. Consequently, the particles become thinner and display and increasing effective elongation $L^*_{ef} = L/\sigma_{ef}$. Temperature is expressed in reduced form as $T^* = k_B T/\epsilon$.

this way, all the thermodynamical and structural properties of the soft model are assimilated to those of the reference hard model. For the case of particles with spherical symmetry, the HS model is usually taken as reference. In the present work, we evaluate the extension of that approach to the characterisation of soft-body SRS rod-like particles. In this case, the HSC fluid constitutes the natural choice of reference potential, and the effective diameter is given by the expression [10]:

$$\sigma_{ef}(T) = \int_0^\infty (1 - \exp[-\beta U_{SRS}(d_m)])\, d(d_m) \qquad (1)$$

where $\beta \equiv k_B T$ (k_B being the Boltzmann constant). According to the above expression, the SRS fluid is mapped onto an HSC fluid with an effective diameter $\sigma_{ef}(T)$ and, correspondingly, an elongation $L^*_{ef}(T) = L/\sigma_{ef}(T)$. Figure 1 provides a schematic representation of the $\sigma_{ef}(T)$ and $L^*_{ef}(T)$ functions over an illustrative range of temperatures. It can be readily observed that the effective diameter of the SRS particles decreases with temperature as a consequence of the greater interpenetration of the particle pairs. Consequently, the elongation of the particles grows with temperature, which in turn has a remarkable effect in the phase diagram of the fluid, as shown below in detail. It should be remarked that the mapping is not dependent on the density of the fluid, which implies that it applies to all the phase states computed for each isotherm. Since solid, liquid crystalline and isotropic phases may occur along each isotherm, the accuracy of a single-parameter SRS–HSC mapping is subjected to a much more complex scenario than for spherical particles and its application can be more subtle and occasionally counter-intuitive. It is important to note that at the temperature $T^* = 1.465$, $\sigma_{ef}/\sigma = 1$, hence the effective HSC fluid has the same diameter and elongation as the ones assigned to the SRS fluid.

For the implementation of the mapping methodology, a good knowledge of the phase diagram of the reference model system is mandatory. For the present investigation, we have relied on the free-energy study of the HSC fluid performed by Bolhuis and Frenkel [28]. That study traced the boundaries of the relevant phases (isotropic, nematic, smectic and solid phases) for a broad range of particle elongations. The mapping methodology is then quite straightforward; the equation of state and phase transitions of an SRS fluid with given values of particle elongation and system temperature, are considered to be those of the HSC fluid of diameter σ_{ef}. Since Bolhuis and Frenkel computed the phase diagram of the HSC fluid for a discrete number of molecular elongations, the estimation of the phase diagram for arbitrary values of the lengths of the molecules involved a certain degree of interpolation and extrapolation of the free-energy data. We do not expect, however, the present results to be severely affected by this limitation.

In [35] the same HSC–SRS mapping defined in Equation (1) was marginally explored to describe the I–N phase transition of the SRS fluid with $L^* = 5$, with good results. In this work, we evaluate more systematically its predictive power over a broad range of particle elongations and system temperatures, leading to layered solid and smectic phases at high densities, and to nematic and isotropic phases at lower densities. The accuracy of the mapping is contrasted against the result of the MC simulations. It is important to note that the comparisons performed in this study between the SRS fluid and its effective HSC counterpart employ the same definition of reduced thermodynamic and physical parameters (e.g. pressures, densities and intermolecular distances), in terms of σ. As the reference HSC fluid is considered with diameter σ_{ef}, the results for it should be rescaled to σ.

2.3. Monte Carlo simulations

The isothermal–isobaric ensemble Monte Carlo (NPT-MC) simulation methodology employed to evaluate the liquid crystal phase diagram of the SRS fluids explored in this work was essentially the same described in previous papers of our group [34,35,38,39]. Isotherms were run for systems of $N_p = 1500$–3000 molecules, depending on molecular elongation so as to ensure that all box sides exceeded the range of the interactions.

Each state was typically equilibrated over more than 10^6 NPT-MC cycles and ensemble averages of the thermodynamic and structural properties of the system were

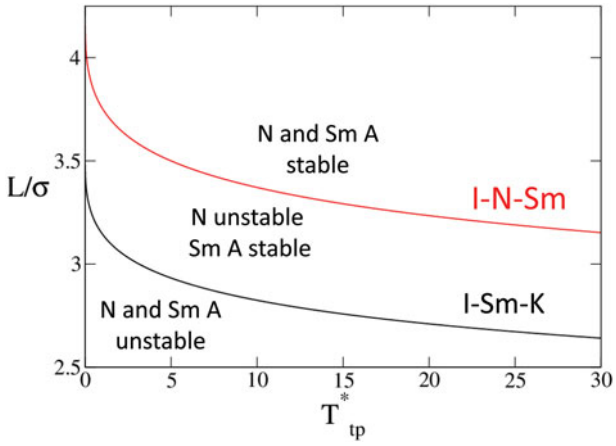

Figure 2. Temperature $T^*_{tp} = k_B Ttp/\epsilon$ of the I-Sm-K triple point (black line) and the I-N-Sm triple point (red line) for SRS fluids of elongation $L^* = L/\sigma$, resulting from the SRS–HSC mapping defined by Equation (2) and the HSC phase diagram of [28]. For a given temperature of the SRS fluid, the smectic and nematic phases are predicted to be stable at temperatures higher than those of the corresponding triple point.

computed over 3×10^5 cycles. Each MC cycle consisted of N_p attempts for displacements and/or reorientations of randomly chosen particles plus a trial change of the box volume. Volume changes were attempted by randomly changing the length of the each side of the box independently. The usual acceptance ratios and periodic boundary conditions are employed.

The computation of each isotherm was started at high pressure with an initial hexatic solid arrangement. The pressure of the fluid was progressively decreased to follow the range of stability of the hexatic solid (K), smectic A (Sm A), nematic (N) and isotropic (I) phases. The phase transitions observed during the isothermal expansion of the fluid were monitored by the changes in density, energy, nematic and bond hexagonal order parameters, and in appropriate radial correlation functions [34,40] Reversed-isotherms performed from back compressions of the fluids from the isotropic phase showed that hysteresis effects were not relevant within the accuracy of our simulations. Such MC procedure for the estimation of liquid crystal phase boundaries is reliable for the purposes of the present work and has been extensively employed in the past for similar fluids of prolate molecules [29,34,40]. A more precise evaluation of the phase diagram should include a calculation of the free energy in each of the phases [28,41] which constitutes a challenge for future studies.

3. Results and discussion

One of the fundamental features of the phase diagram of the HSC fluid is the limitation established by the elongation of the particles to the existence of the different liquid crystalline phases. Specifically, the smectic and the nematic phases become only stable for HSC rods longer than $L^* = 3.1$ and longer than $L^* = 3.7$, respectively [28]. In the SRS fluid, phase stability is as well modulated by temperature, a parameter not explicitly relevant for the HSC fluid.

The SRS–HSC mapping method serves in fact to predict the temperature of the isotropic–smectic–solid (I-Sm-K) and the isotropic–nematic–smectic (I-N-Sm) triple points for SRS fluids of given particle elongations. This is accomplished, for each value of L/σ, through the calculation with Equation (1) of the temperatures at which the effective length of the particles becomes $L^*_{ef} = 3.1$ (I-Sm-K triple point) and $L^*_{ef} = 3.7$ (I-N-Sm triple point). The temperatures thus obtained for the two triple points are represented in Figure 2. From these temperatures, an overall description of the topology of the liquid crystal phase diagram at a given elongation L^* of the SRS particles can be inferred. The nematic and smectic phases are only stable at temperatures higher than those delimited by the I-N-K

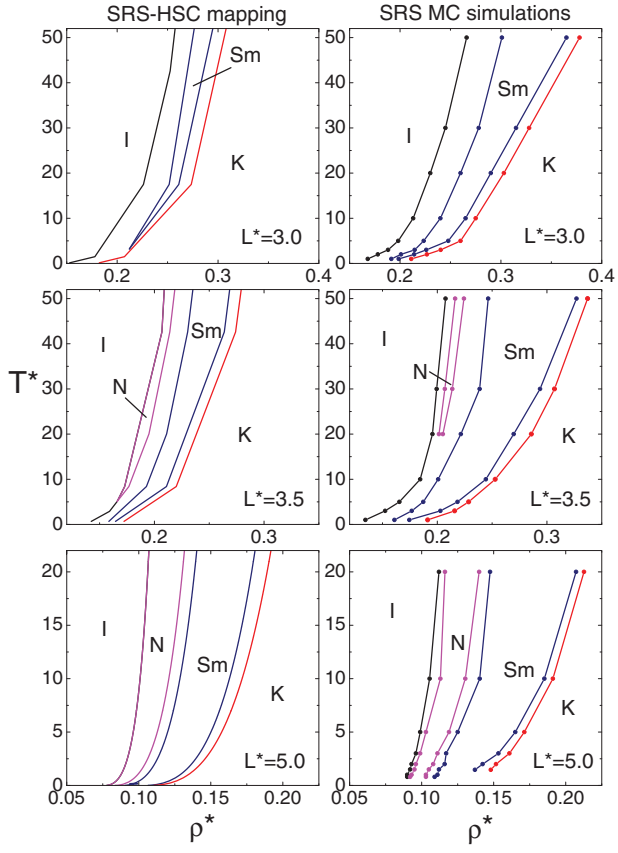

Figure 3. Liquid crystal phase diagrams obtained from MC simulations (right-hand panels) and predicted by the SRS–HSC mapping (left-hand panels) for SRS fluids with three elongations, $L = 3$, 3.5 and 5. These elongations are illustrative of the three regimes of liquid crystal behaviour described by the triple point curves depicted in Figure 2. The curves represent the boundary states defining the transitions between the solid (K), smectic (Sm), nematic (N) and isotropic (I) phases of the fluids.

and I-Sm-K lines in Figure 2, respectively. This leads to three distinct ranges of rod elongations with qualitatively different liquid crystalline behaviour.

Figure 3 illustrates such ranges by displaying the phase diagrams predicted by the mapping for a selection of L^* values. The first range includes the SRS particles with high elongations, namely $L^* > 3.7 \times 2^{1/6} = 4.15$ (the factor $2^{1/6}$ represents the maximum value that $\sigma^*_{\rm eff}/\sigma$ takes in the low temperature limit, according to Equation (1)). The phase diagram of these fluids does not show triple points, so that the isotropic, nematic, smectic and solid phases may be found at any temperature, at appropriate densities of the system. A second range applies to intermediate elongations, $4.15 > L/\sigma > 3.1 \times 2^{1/6} = 3.48$. In this case, only an I-N-K triple point is predicted, meaning that the smectic phase is stable at all temperatures, while the nematic phase becomes stable only at sufficiently high temperature. For instance, for $L^*=3.5$, in an isothermal compression at low temperature, the fluid would undergo subsequent isotropic–smectic and smectic–solid transitions. The nematic phase emerges however at temperatures above $T^* \approx 4.8$, leading to isotropic–nematic and nematic–smectic transitions. Finally, the third range is related to short elongations, $L/\sigma < 3.1 \times 2^{1/6} = 3.48$. In this case, both I-Sm-K and I-N-Sm triple points are predicted to be present in the liquid crystalline phase diagram, so that the stability of both the nematic and smectic mesophases is subjected to temperature. At low temperature none of them is stable, leading to an isotropic–solid transition without liquid crystalline behaviour. At intermediate temperatures, the smectic phase becomes stable and at high temperatures the nematic phase is also incorporated.

It must be noted that within the SRS–HSC mapping, the rod-like particles can in principle become arbitrarily thin

Table 1. Densities, ρ^*, of the phase boundary states obtained in the present MC simulations for SRS fluids with the indicated elongations, L^*, and temperatures, T^*. All values are given to the last statistically significant digit.

$T^*=$	50	30	20	10	5	3	2	1.465	1	Phase
$L=7$					0.1278	0.1186	0.1163			H
					0.1211	0.1124	0.1090			Sm
					0.0907	0.0820	0.0815			Sm
					0.0831	0.0737	0.0687			N
					0.0581	0.0570	0.0563			N
					0.0476	0.0460	0.0432			I
$L=5$			0.2127	0.1911	0.1713	0.1609	0.1516	0.1480		H
			0.2072	0.1852	0.1650	0.1533	0.1423	0.1370		Sm
			0.1475	0.1403	0.1295	0.1240	0.1246	0.1114		Sm
			0.1399	0.1303	0.1194	0.1112	0.1085	0.1015		N
			0.1162	0.1130	0.1019	0.1011	0.0990	0.0963		N
			0.1110	0.1055	0.0985	0.0944	0.0920	0.0920		I
$L=4$			0.2637	0.2307	0.2080	0.1950	0.1811	0.1740		H
			0.2510	0.2248	0.1998	0.1830	0.1710	0.1618		Sm
			0.1993	0.1758	0.1627	0.1600	0.1533	0.1482		Sm
			0.1773	0.1600	0.1500	0.1422	0.1369			N
			0.1670	0.1511	0.1456	0.1401	0.1355			N
			0.1603	0.1497	0.1409	0.1373	0.1310	0.1304		I
$L=3.5$	0.3371	0.3069	0.2858	0.2528	0.2286	0.2158			0.1912	H
	0.3270	0.2937	0.2697	0.2443	0.2184	0.2028			0.1745	Sm
	0.2464	0.2386	0.2215	0.2008	0.1872	0.1767			0.1609	Sm
	0.2243	0.2137	0.2051							N
	0.2163	0.2069	0.2015							N
	0.2075	0.1994	0.1956	0.1844	0.1654	0.1524			0.1344	I
$L=3.25$	0.3522	0.3250	0.3062	0.2705	0.2415					H
	0.3437	0.3116	0.2897	0.2613	0.2307					Sm
	0.2688	0.2556	0.2417	0.2194	0.2041					Sm
	0.2572									N
	0.2459									N
	0.2409	0.2211	0.2110	0.1969	0.1812					I
$L=3$	0.378	0.328	0.303	0.275	0.260	0.240	0.227		0.211	H
	0.365	0.315	0.289	0.265	0.248	0.226	0.214		0.199	Sm
	0.301	0.278	0.261	0.241	0.224	0.215	0.201		0.192	Sm
	0.266	0.245	0.232	0.213	0.198	0.188	0.178		0.168	I
$L=2$	0.456		0.3973		0.347	0.324	0.308			H
	0.405		0.3535		0.300	0.279	0.264			I

and elongated at high temperature ($\sigma_{ef}(T)$ decreases, and hence $L^*_{ef}(T)$ increases, monotonously with T). It would seem that, contrary to the HSC fluid, the adjustment of temperature in the SRS fluid allows to modulate the stability of the nematic and smectic phases at any elongation. While this is formally true, for short SRS rods, the temperatures at which the triple points are located eventually become too large and unrealistic to model real fluids. For instance, for the SRS fluid with $L^* = 2.5$ the mapping predicts the emergence of the smectic and the nematic phases at $T^* > 60$ and $T^* > 500$, respectively (see Table 1).

Figure 3 and Table 1 summarise the limits of the phase transitions resulting from the MC simulations and compare them with the corresponding predictions of the SRS–HSC mapping. Such comparison considers particle elongations ranging $L^*= 2$–7, thereby including the three regimes of triple points described above. Moreover, an ample range of temperatures has been explored in order to evaluate isothermal expansions through qualitatively different regions of the phase diagram at each elongation. There is an overall qualitative agreement between the phase diagrams obtained in the MC simulations and those predicted by the SRS–HSC mapping. At low particle elongations, e.g. $L^*= 2$, no liquid crystalline behaviour is observed, and the solid melts directly to an isotropic fluid. At greater elongations, the smectic phase becomes eventually stable. In fact, this phase was present in all the isotherms computed in our study for fluids with $L^* \geq 3$. Whereas this finding is in good agreement with the predictions of the SRS–HSC mapping, the I-Sm A-K triple point derived from the simulations seems to lie significantly lower in temperature. For instance, the MC simulations for the SRS fluid with $L^*= 3$ indicate that such triple point is located at $T^*<1$, while the mapping predicts a temperature of $T^* \approx 3$. For $L^* > 3$, the MC and the mapping data agree well in the absence of the I-Sm A-K triple point, meaning that the smectic phase is stable in ranges of densities at all temperatures, as can be seen in Figure 3. As for the nematic phase, the MC study finds regimes of stability for all the SRS fluids with $L^*\geq 3.25$, emerging at progressively lower temperatures as the elongation is increased. For $L^*= 3.5$ the nematic phase is observed at $T^*\geq 20$, for $L^*= 4$ at $T^*\geq 2$ and for $L^*\geq 5$ at all values of T^*. Whereas this trend is again in concordance with the prediction of the SRS–HSC mapping, this latter approach leads to significantly broader ranges of stability of the nematic phase and to a I-N-Sm A triple point lower in temperature, in comparison to the MC simulations.

In conclusion, in comparison to the MC simulations, the SRS–HSC mapping overestimates the temperature of the I-Sm-K triple point and, on the contrary, it underestimates the temperature of the I-N-Sm triple point. In other words, the representation of the soft SRS interactions with effective hard-bodies tends to favour the stability of the nematic phase and to hinder that of the smectic phase.

At this point, we perform a closer evaluation of the performance of the SRS–HSC mapping, in terms of isotherms and radial functions obtained in MC simulations for SRS fluids and for their effective HSC counterparts. We will focus on the SRS fluid with $L^*= 5$, and will consider three illustrative temperatures, namely $T^*= 1.465$, 5.0 and 20.0. According to the mapping defined by Equation (1), the effective HSC fluids corresponding to those temperatures have elongations $L^*_{ef} = 5.000$, 5.286 and 5.721, respectively. Figure 4 compares the EOS of these SRS and HSC fluids, obtained in the MC simulations. All isotherms correspond to expansions of the hexatic solids through the smectic and nematic liquid crystal phases to the isotropic phase. Figure 5 shows the radial functions, $g(r)$, for SRS and HSC states of similar packing fraction, within the solid, smectic and nematic phases of these fluids.

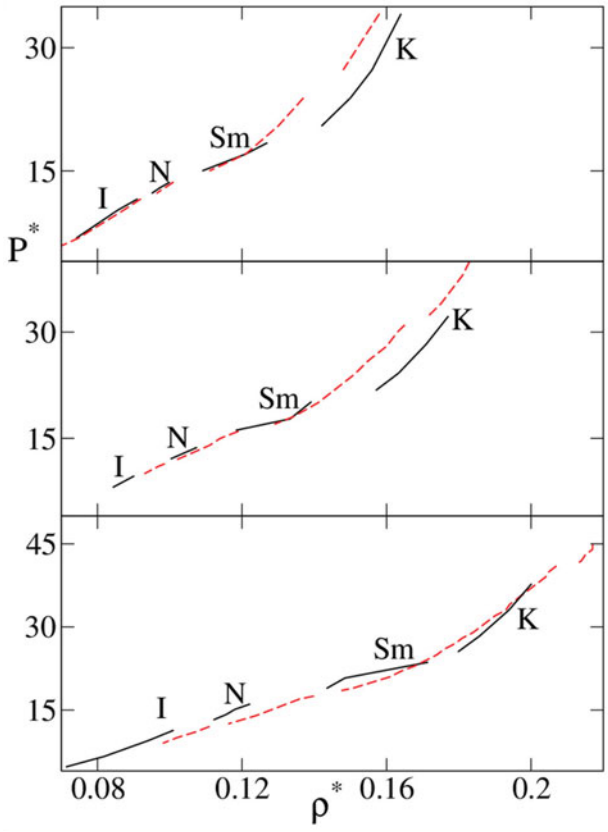

Figure 4. Equations of state obtained in MC simulations for the SRS fluid (solid lines) with $L^*= 5$ at temperatures $T^*= 1.465$ (top), 5.0 (middle) and 20.0 (bottom), compared to those obtained with the same method for HSC fluids (dashed lines) with the elongations $L^*= 5.000$, 5.286 and 5.721, respectively.

In general terms, there is a fairly good coincidence in the EOS and radial functions of the SRS and of the corresponding effective HSC fluids, especially within the isotropic, nematic and smectic phases. The differences between the two fluids become more evident as the temperature is increased, especially in the solid phase where the SRS fluid is more highly packed and displays sharper peaks in the radial distribution function than the HSC fluid. In any case, this level of discrepancy for states of high density is not

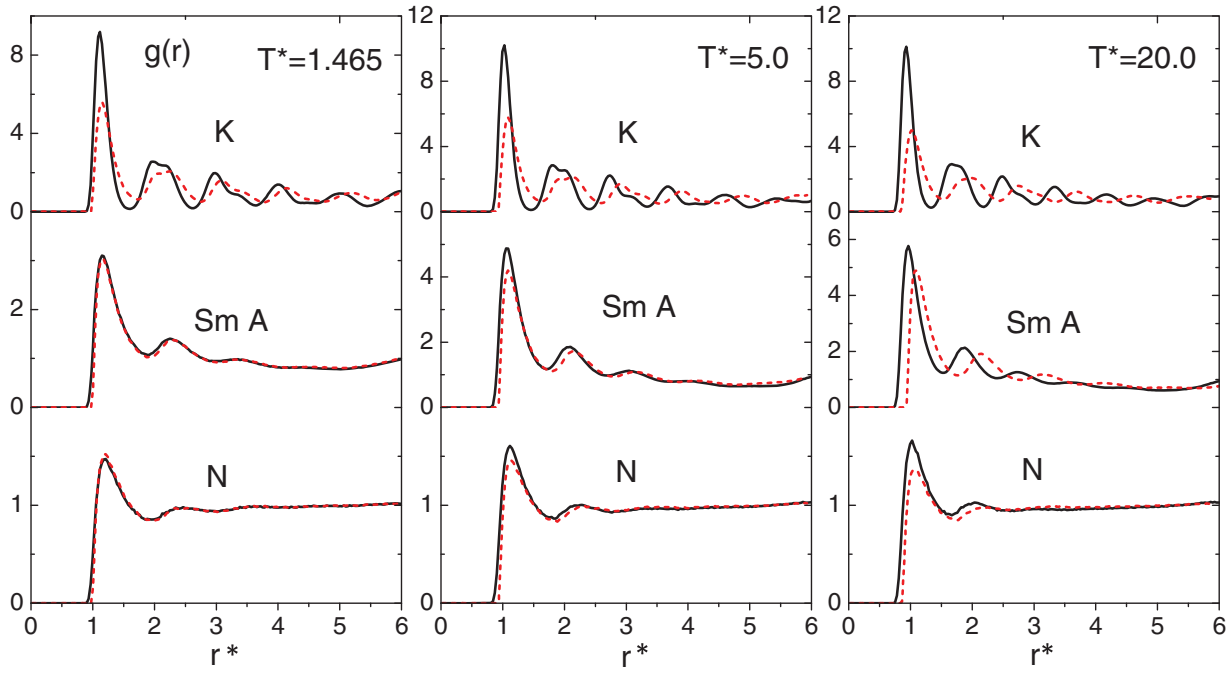

Figure 5. Radial functions obtained in MC simulations for the SRS fluid (solid lines) with $L^*= 5$ at temperatures $T^*= 1.465$, 5.0 and 20.0, compared to those obtained with the same method for HSC fluids (dashed lines) with the elongations $L^*= 5.000$, 5.286 and 5.721, respectively.

entirely unexpected, in particular taking into account that the mapping is based on a single (temperature-dependent) parameter that originates, as introduced by Boublik, from an expansion of a reference partition function only up to second order. For soft bodies the Boltzmann factor associated with the interpenetration of the pairs of particles grows rapidly with increasing temperature, and this feature is intended to be captured by expression for σ_{ef} described in Equation (1). The present study shows in fact that such expression actually works quite accurately over a broad range of temperatures, densities and liquid crystalline phases. Its limitations are only exposed at high temperature and at the high packing fractions and tight arrangements typical of the solid phase.

4. Summary and conclusions

The liquid crystalline behaviour of the soft repulsive SRS fluid for rod-like particles has been characterised by means of MC simulations over ample ranges of particle elongations and system temperatures and densities. The description of this fluid should be useful for future developments in which a continuous and fully derivable reference interaction potential is required.

The simulations have served to illustrate the role of temperature in determining the stability of the nematic and smectic phases of these fluids, something that was not possible explicitly with the well -known HSC fluid. It has been shown in particular that the introduction of temperature induces the appearance of isotropic–nematic–smectic and isotropic–smectic–solid triple points in the phase diagrams of systems of particles of given elongations.

In order to rationalise in more depth these features, a mapping of the SRS fluids on effective HSC fluids has been performed, that is in line with previous developments of Boublik and others for related systems. One main advantage of such mapping is that perturbative approaches may benefit from the use of hard-body potentials that resemble the behaviour of specific soft-body systems with sufficient accuracy. The mapping is based on the assignment of an effective hard-core size based on the thermal interpenetration of the pairs of particles. Hence, an effective diameter is defined that depends solely on temperature. In spite of the simplicity of this approach, this study has shown that it describes fairly well the characteristics of the SRS fluid, in particular within the nematic and smectic liquid crystal phases. Among the limitations of the mapping revealed in our study, the overestimation of the stability of the nematic phase and the underestimation of that of the smectic phase, with respect to the MC simulations, are worth mentioning. In addition, the description of the SRS fluid at high temperature and in the solid phase is not well accounted for by the mapping. Keeping in mind these limitations, the procedure presented in this paper provides a valuable route to obtain basic information about the topological shape of the phase diagram of any soft repulsive model.

Funding

The research activity of our group is currently supported by the Government of Spain [projects CTQ2012-32345 and Consolider-Ingenio CSD2009-00038], and by Junta de Andalucía-FEDER [project P12-FQM-4938].

References

[1] D.A. McQuarrie, *Statistical Mechanics* (University Science Books, Susalito, 2000).
[2] J.A. Barker and D. Henderson, J. Chem. Phys. **47**, 4714 (1967).
[3] N.F. Carnahan and K.E. Starling, J. Chem. Phys. **51**, 635 (1969).
[4] Z. Chenga, P.M. Chaikina, W.B. Russelb, W.V. Meyerc, J. Zhub, R.B. Rogersc, and R.H. Ottewilld, Mater. Des. **22**, 529 (2001).
[5] J.D. Weeks, D. Chandler, and H.C. Andersen, J. Chem. Phys. **54**, 5237 (1971).
[6] J. Fischer and S. Lago, J. Chem. Phys. **78**, 5750 (1983).
[7] M. Bohm, S. Lago, and J. Fischer, Fluid Phase Equil. **23**, 137 (1985).
[8] T. Boublik, Coll. Czech. Chem. Commun. **39**, 2333 (1974).
[9] T. Boublik, Mol. Phys. **27**, 1415 (1974).
[10] T. Boublik, Mol. Phys. **32**, 1737 (1976).
[11] T. Boublik, J. Chem. Phys. **87**, 1751 (1987).
[12] T. Boublik, J. Chem. Phys. **9**, 4084 (1975).
[13] T. Boublik and I. Nezbeda, Coll. Czech. Chem. Commun. **51**, 2301 (1974).
[14] T. Boublik, I. Nezbeda, and O. Trnka, Czech. J. Phys. B **26**, 1081 (1976).
[15] R. Kantor and T. Boublik, Mol. Sim. **2**, 217 (1989).
[16] S. Lago and T. Boublik, Coll. Czech. Chem. Commun. **45**, 3051 (1980).
[17] J. Pavlicek, J. Aim, and T. Boublik, Fluid Phase Equil. **91**, 203 (1993).
[18] T. Boublik, J. Phys. Chem. **92**, 2629 (1988).
[19] T. Boublik, Fluid Phase Equil. **1**, 37 (1977).
[20] P.G. de Gennes and J. Prost, *The Physics of Liquid Crystals*, 2nded. (Clarendon Press, Oxford, 1993).
[21] L. Onsager, Ann. N.Y. Acad. Sci. **51**, 627 (1949).
[22] S.C. McGrother, D.C. Williamson, and G. Jackson, J. Chem. Phys. **104**, 6755 (1996).
[23] M. Franco-Melgar, A.J. Haslam, and G. Jackson, Mol. Phys. **106**, 649 (2008).
[24] D. Frenkel and B.M. Mulder, Mol. Phys. **55**, 1171 (1985).
[25] J.G. Gay and B.J. Berne, J. Chem. Phys. **74**, 3316 (1981).
[26] L.F. Rull, Phys. A **220**, 113 (1995).
[27] C. Zannoni, J. Mater. Chem. **11**, 2637 (2001).
[28] P. Bolhuis and D. Frenkel, J. Chem. Phys. **106**, 666 (1997).
[29] A. Cuetos, B. Martínez-Haya, S. Lago, and L.F. Rull, Phys. Rev. E **68**, 011704 (2003).
[30] K.M. Aoki and T. Akiyama, Mol. Sim. **16**, 99 (1996).
[31] K.M. Aoki and T. Akiyama, Mol. Cryst. Liq. Cryst. **299**, 45 (1997).
[32] M.S. Al-Barwani and M.P. Allen, Phys. Rev. E **62**, 6706 (200).
[33] D.J. Earl, J. M. Ilnytskyi, and M.R. Wilson, Mol. Phys. **99**, 1719 (2001).
[34] A. Cuetos, B. Martínez-Haya, L.F. Rull, and S. Lago, J. Chem. Phys. **117**, 2934 (2002).
[35] A. Cuetos, B. Martínez-Haya, S. Lago, and L.F. Rull, J. Phys. Chem. B **109**, 13729 (2005).
[36] A. Patti and A. Cuetos, Phys. Rev. E **86**, 011403 (2012).
[37] C. Vega and S. Lago, Comput. Chem. **18**, 55 (1994).
[38] B. Martínez-Haya and A. Cuetos, J. Phys. Chem. B **111**, 8150 (2007).
[39] B. Martínez-Haya, A. Cuetos, S. Lago, and L.F. Rull, J. Chem. Phys. **122**, 024908.26 (2005).
[40] B. Martínez-Haya and A. Cuetos, J. Chem. Phys. **131**, 074901 (2009).
[41] M. Marechal, A. Cuetos, B. Martínez-Haya, and M. Dijkstra, J. Chem. Phys. **134**, 094501 (2011).